Complete odometry estimation of a vehicle using single automotive Radar and a gyroscope

Reza Ghabcheloo, Shadman Siddiqui

Abstract— In this paper, we propose an algorithm for complete odometry of a vehicle on a horizontal plane, that is, estimation of linear velocity vector (forward and sideslip speeds) and angular speed of a vehicle. The vehicle is equipped with an automotive Radar sensor and a vertical gyro. The Radar sensor provides radial speed and azimuth angle of number of objects in the environment. We first derive the kinematic constraints imposed on the vehicle motion and stationary points in the environment. Using the constraints we classify the points detected by the Radar to stationary and non-stationary points. It is known that using data from a single Radar, the above-mentioned constraints are singular. Previous works have thus proposed the use of more than one Radar sensor, or they have neglected the sideslip speed. In our work, we then use the Radar data of the stationary objects and a gyro data to solve an optimization algorithm to calculate vehicle odometry. Experimentation has been performed with a non-road vehicle driven on a straight path and on a circular path. We report our findings and show efficacy of the algorithm in comparison to the state of art [8] as well as wheel odometry and a complete navigation solution (including GNSS) as the reference path.

I. INTRODUCTION

Odometry/ego-motion estimation is a widely studied and important topic in field of mobile robotics. There are two different methods to perform this task: which are 1) proprioceptive or absolute position sensors such as wheel speeds, IMUs and GNSS[1]; and the other is based on 2) exteroceptive sensors, most common is visual odometry [2].

The basic principle of wheel odometry is to convert wheel revolution to linear displacement. However, due to sliding and skidding of the wheels, this conversion contains errors. These errors can be categorized into two groups, 1) systematic errors, which are due to kinematic imperfections of the vehicle, and 2) non-systematic errors, which are due to the terrain on which the vehicle is moving, caused by sideslip, wheel slippage, cracks and bumps. Commonly used odometry is fusion of wheel odometry and IMUs. The errors are then compensated using GNSS or landmark fixes, but one or more than one major non-systematic error can make these systems fail [7].

The aim of this research is to provide a redundant solution for common odometry methods. We will devise an estimation algorithms to a complete odometry of a vehicle using automotive Radar and a gyro. This approach falls under the exteroceptive sensors method. However, instead of visual cameras we use Radar. Usability of our method is growing as the Radar sensors are becoming commonplace in the modern vehicles and mobile machines is growing and they are robust to weather conditions.
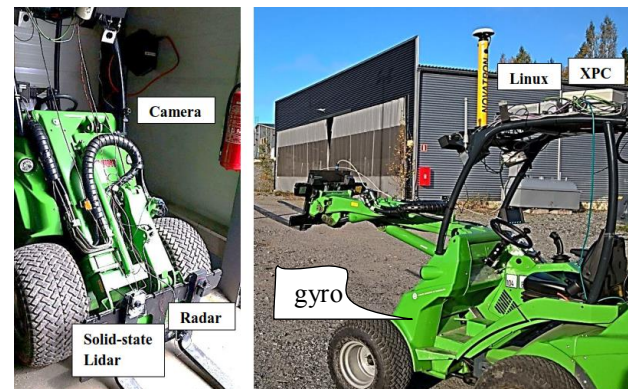

Figure 1 Test platform (GIM mobile machine)

The vehicle for testing purposes in this research is a multipurpose wheel loader based on Avant 635 that was built at the Laboratory of Automation and Hydraulics (AUT), Tampere University of Technology (TUT), under the Generic Intelligent machine (GIM) project [1], see Figure 1. It is an articulated-frame-steering hydraulically actuated mobile machine. This machine is hereafter referred to as the GIM mobile machine. Current navigation system on GIM mobile machine is based on wheel odometry, IMU and GNSS [4].

The problem of odometry on a plane is about computation of linear velocity vector (2 components) and angular speed (1 component). We study the problem in two cases: 1) the general case (computing all 3 components); 2) where sideslip or drift is negligible, thus only calculating one variable for linear speed. The Radar sensor detects objects in a range of 80 m, and base on the reflection it returns information of radial speed, radial distance, probability of the object, azimuth angle. Moreover, the sensor can detect up to 32 objects in a single measurement cycle. In our work, we only use the radial speed and the azimuth angle. Mounting pose (position and orientation) of the sensor frame relative to the body frame is also needed. In our case, the IMU frame is chosen as the body frame.

Authors are with the Laboratory of Automation and Hydraulics (AUT), Tampere University of Technology (TUT). Tampere, Finland.

Emails: first name.last name@tut.fi; Corresponding author reza.ghabcheloo@tut.fi

[1] Inertial Measurement Unit and Global Navigation Satellite System

In [4], an improved odometry algorithm is proposed for the GIM mobile machine. Hall sensors are installed on all four wheels. A generalized least-square estimator is used to reduce errors of the odometry. The method reduced the errors of angular velocity estimates, but only slight improvement in linear speed estimation. Several other works use wheel speeds based odometry for vehicles [5] and [12].

In [6], Vivet et al. proposed a technique of using a rotating Radar sensor (K2PI) to calculate the linear and angular speed of the vehicle. The data collected from rotating range sensors contains distortion. The use of slow rotating sensor limits the application for low speed vehicle at most to 30 km/hr. In [13], Checchin et al. proposed a technique for SLAM (Simultaneous Localization and Mapping) using a rotating Radar sensor based on FMCW (Frequency Modulated Continuous Wave). For odometry estimation, they used Fourier Mellin Transform, registering the images of the Radar sensor in a sequence.

In [8], Kellner et al. proposed an instantaneous ego motion estimation technique using Doppler Radar sensors. Ackermann conditions were assumed. The authors used Random Sample Consensus (RANSAC) technique to remove moving objects from the data. They used multiple Doppler Radar sensors. Limitation of this technique is that it cannot be applied to non-Ackermann steered platforms. We will compare our solution to theirs.

In [9], a probabilistic approach for ego-motion estimation using single and multiple Doppler Radar and the vehicle kinematic equations has been presented. Normal distribution transform (NDT) is utilized for optimum position matching of detections. The experiments are performed using stereo Doppler Radar and the results are compared with vehicle odometry and high precision IMUs. In [10], Corominas-Mutra et al. continued the work presented in [9] and proposed a method for optimal sensor placement and estimating the odometry of the vehicle. Corominas-Mutra et al also showed that calculation of complete odometry estimation (all 3 components) is not possible with a single Radar sensor and stereo Radar sensors placed in optimal places can estimate the odometry of the vehicle.

TABLE I.   REVIEW OF TECHNIQUES USED FOR RADAR ODOMETRY ESTIMATION

Sensors	Technique	Side slip included	Ref.
Single Radar	Ackermann conditions/RANSAC	No	[8]
Multiple Radar	Ackermann conditions/RANSAC	Yes	[14]
Stereo Radar	Kinematic equation/ Normal Distribution Transform	Yes	[9]
Stereo Radar	Kinematic equation/optimal placement of Radar	Yes	[19]
Single Radar + gyroscope	Kinematic equation/RANSAC	Yes	This work

The algorithm proposed in this paper can be applied to both Ackermann and non-Ackermann vehicles. Moreover, in this research single Radar and a gyro is used for complete odometry estimation including sideslip. In our solution, use of more than one Radar sensor is possible. Table 1 presents a review of the techniques used for Radar sensor based odometry.

The paper is organized as follows. Section II presents the kinematic model to be used in our odometry estimation. It consists of two cases, 1) estimation of odometry with sideslip, and 2) estimation of odometry without sideslip. Section III states the algorithm for estimation of odometry. The experimentation is presented in section IV. In the section V, complete navigation solution (wheel odo, IMU, GNSS) is used as a reference. In the case of ego-motion estimation without sideslip, the results have been compared with [8] and our improved wheel odometry system. Section VI concludes the paper.

II. MATHEMATICAL MODELING

Radar sensor provides distance measurements from certain number of objects in the field of view of the sensor, relative radial velocity of the objects, the angle at which the object is present relative to the Radar frame. Our objective is to develop an algorithm to estimate linear speed, angular speed and sideslip (side speed) of the GIM mobile machine on which the Radar is mounted.

Next, we derive the kinematic constraints between the vehicle motion and a stationary point in the environment. Assuming p_i is a stationary point in the environment, we will calculate the two components of linear velocity vector and a single component of angular speed relative to the body frame as shown in Figure 2. Let's define body frame {B} (OXYZ) and Radar sensor frame {R} (OXYZ), object 'p_i' with $i = 1....n$, where n is the object index. The motion of the machine is measured in a world frame {W} (OXYZ). We also define end frame {E_i}(OXYZ). E_i and R have the same origin, while x_E faces towards the object p_i.
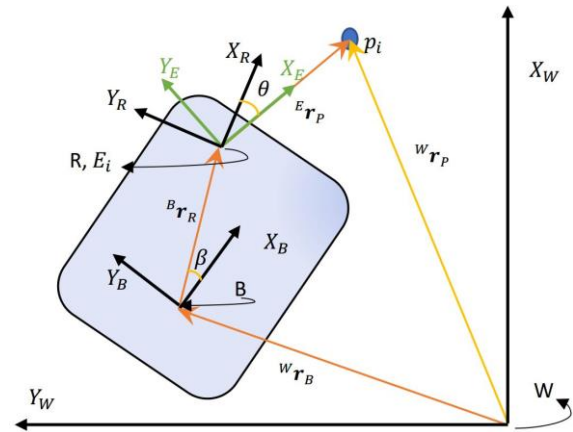

Figure 2:Point P represented in Radar Frame R, Body frame B and World Frame W, and their origins O_R, etc. Note: Positive rotation is counter clockwise and z-axis up

The following equation describes constraints among the frames

$${}^W\boldsymbol{r}_p = {}^W\boldsymbol{r}_B + {}^W\boldsymbol{R}_B \, {}^B\boldsymbol{r}_R + {}^W\boldsymbol{R}_B \, {}^B\boldsymbol{R}_R \, {}^R\boldsymbol{R}_E \, {}^E\boldsymbol{r}_p \tag{1}$$

where ${}^W\boldsymbol{r}_p$ is the position of p_i in W expressed in W. We have dropped the index i for the sake of clarity of presentation. ${}^W\boldsymbol{r}_B$ is the position of O_B in W expressed in W. ${}^W\boldsymbol{R}_B$ is the rotation matrix from B to W. Variable ${}^B\boldsymbol{r}_R$, ${}^R\boldsymbol{R}_E$, and ${}^E\boldsymbol{r}_p$ are defined in a similar manner. Differentiation of (1) results in

$${}^W\dot{\boldsymbol{r}}_p = {}^W\dot{\boldsymbol{r}}_B + {}^W\dot{\boldsymbol{R}}_B \, {}^B\boldsymbol{r}_R + {}^W\boldsymbol{R}_B \, {}^B\dot{\boldsymbol{r}}_R + {}^W\dot{\boldsymbol{R}}_B \, {}^B\boldsymbol{R}_R \, {}^R\boldsymbol{R}_E \, {}^E\boldsymbol{r}_p + {}^W\boldsymbol{R}_B \, {}^B\boldsymbol{R}_R \, {}^R\dot{\boldsymbol{R}}_E \, {}^E\boldsymbol{r}_p + {}^W\boldsymbol{R}_B \, {}^B\boldsymbol{R}_R \, {}^R\boldsymbol{R}_E \, {}^E\dot{\boldsymbol{r}}_p \tag{2}$$

A. CASE 1: Calculating linear speed, angular speed, and sideslip

After some manipulation, equation (2) simplifies to

$$\begin{bmatrix} 0 \\ 0 \end{bmatrix} = \begin{bmatrix} v_B \\ v_d \end{bmatrix} + \omega_B \begin{bmatrix} -y_B \\ x_B \end{bmatrix} + \omega_B \begin{bmatrix} -d_i \sin(\theta + \beta) \\ d_i \cos(\theta + \beta) \end{bmatrix}$$
$$+ \dot{\theta} \begin{bmatrix} -d\sin(\theta + \beta) \\ d\cos(\theta + \beta) \end{bmatrix} - \begin{bmatrix} v_r \cos(\theta + \beta) \\ v_r \sin(\theta + \beta) \end{bmatrix} \tag{3}$$

where v_B, v_d and ω_B are the unknown components of linear forward speed, sideslip speed, and angular speed, respectively; x_B and y_B are the longitudinal and lateral position of the Radar sensor in the Body frame; β is the orientation angle at which the Radar sensor is mounted. Variables d, θ and v_r are the range, azimuth angle, and radial velocity of the object detected by the Radar sensor. $\dot{\theta}$ is the change in the azimuth angle and is not of interest. Removing $\dot{\theta}$ from the equations and solving the equation further we get

$$v_B \cos(\varphi) + v_d \sin(\varphi) + \omega_B \big(x_B \sin(\varphi) - y_B \cos(\varphi)\big) - v_r = 0 \tag{4}$$

where $\varphi = (\theta + \beta)$. Adding the object indices to (4), we get

$$v_B \cos(\varphi_i) + v_d \sin(\varphi_i) + \omega_B \big(x_B \sin(\varphi_i) - y_B \cos(\varphi_i)\big) = v_{ri} \tag{5}$$

Notice that (5) is linear in unknowns variables. Using a single Radar and 3 points, we can thus write $= J\boldsymbol{b} + \boldsymbol{\epsilon}$, where $\boldsymbol{b} = (v_B, v_d, \omega_B)^T$ is the vector of unknown variables, $\boldsymbol{\epsilon}$ is the noise sensor noise, and $\boldsymbol{y} = (v_{r1}, v_{r2}, v_{r3})^T$ and

$$J = \begin{bmatrix} \cos(\varphi_1) & \sin(\varphi_1) & -y_B \cos(\varphi_1) + x_B \sin(\varphi_1) \\ \cos(\varphi_2) & \sin(\varphi_2) & -y_B \cos(\varphi_2) + x_B \sin(\varphi_2) \\ \cos(\varphi_3) & \sin(\varphi_3) & -y_B \cos(\varphi_3) + x_B \sin(\varphi_3) \end{bmatrix} \tag{6}$$

This matrix is rank deficient because the last column is a linear combination of first two. Adding more points does not resolve singularity of J. Therefore, the three components of odometry cannot be computed using single Radar sensor, as it is also noted in [10] following similar steps. Previous works have thus proposed the use of more than one Radar sensor [10], or they have neglected the sideslip speed [8]. In our work, we use a vertical gyro to overcome the singularity. This choice is justified since MEMS gyros are readily available [4]

and much cheaper than a second automotive Radar sensor. Therefore in our algorithm for 2 detected points and gyro measurement ω_g, we have $\boldsymbol{y} = (v_{r1}, v_{r2}, \omega_g)^T$ and

$$J = \begin{bmatrix} \cos(\varphi_1) & \sin(\varphi_1) & -y_B \cos(\varphi_1) + x_B \sin(\varphi_1) \\ \cos(\varphi_2) & \sin(\varphi_2) & -y_B \cos(\varphi_2) + x_B \sin(\varphi_2) \\ 0 & 0 & 1 \end{bmatrix} \tag{7}$$

B. CASE 2: Calculating linear and angular speed neglecting side slip

For the case where the sideslip is insignificant, we can neglect the sideslip, that is, $v_d = 0$ and equation (6) can be rewritten as

$$v_B \cos(\varphi_i) + \omega_B \big(x_B \sin(\varphi_i) - y_B \cos(\varphi_i)\big) = v_{ri} \tag{8}$$

In the equation (8), we have two unknowns, and the system of equations (8) can be solved with at least two detected points (not located on the same azimuth angle, that is, $\varphi_i \neq \varphi_j$), and the resulting regression matrix is non-singular even without gyro input.

III. PROPOSED ALGORITHM

Based on the discussion above, in our algorithm we need at least 2 points. We thus propose the following algorithm.

Proposed algorithm:

1. Pick any pair of points (i, j) with non-aligned azimuth angle, that is, $\left|\varphi_i - \varphi_j\right| > \epsilon$, where ϵ is a small value.
2. Calculate triple $\boldsymbol{b} = (v_B, v_d, \omega_B)$ for all possible combinations of pairs $\boldsymbol{b}_k : k = 1, \ldots$
3. Remove the outliers from $\boldsymbol{b}_k$ using RANSAC (RANdom SAmple Consensus)
4. Average the remaining

The logic behind the algorithm is that in ideal case any two points must lead to the same result. However, in reality, due to noise and presence of moving objects, the results do not agree. RANSAC is applied to remove the outliers [11].

Remark: As expected, constraint equations are not dependent on the positions of the objects nor on the heading angle of the machine. Also note that for the algorithm to work, most of the detected objects must be stationary.

IV. EXPERIMENTATION

The sensors on the GIM mobile machine are connected to a Linux PC running ROS (Robot Operating System). Experiments are performed at the TUT Autonomous Test Area (TUT-ATA). The Radar was mounted in front of the machine as shown in Figure 1. The test trajectories were a straight line and a curve line. The data was recorded in ROS and later loaded in MATLAB for processing.

During the tests maximum number of objects detected was 21. After pre-processing, the number of objects detected was normally between 10 to 12. In pre-preprocessing we used a

threshold on the probability of the object and number of times an object was detected (at least two times).

A. Measuring Linear and angular speed neglecting the sideslip

In Figure 3, comparison of Radar odometry and the wheel odometry data is performed. The GIM mobile machine is driven straight forward and then stopped at second 173, and driven backwards. In the linear speed graph, there are few
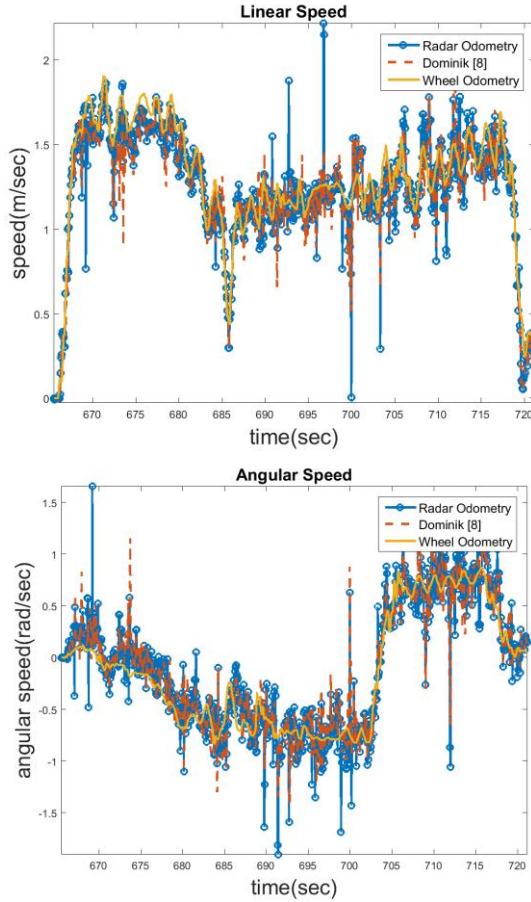

Figure 4: Linear and angular speed of the GIM mobile machine, comparison of this work with Dominik [8] technique and wheel odometry

noisy peaks. However, the trend is quite similar to that of the wheel odometry. Whereas in the angular speed graph, the noise of proposed algorithm is quite high.

Figure 4 shows the comparison of proposed algorithm with [8] and the wheel odometry with the machine moving in the circular path. It is evident that Radar odometry and the [8] technique are quite similar. On the circular path, the GIM mobile machine was first driven counter clockwise and then clockwise, which can be observed in the angular speed graph. Note that equations in [8] are driven based on Ackermann constraints, while GIM mobile machine is not Ackerman steered; it is a so called articulated frame steered. Moreover, the proposed algorithm assumes negligible sideslip, which was not a valid assumption for the test driving condition.
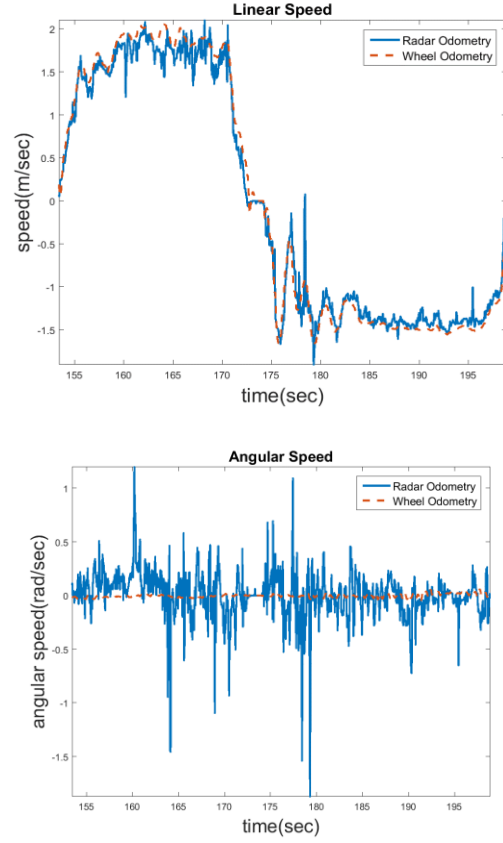

Figure 3: Linear and angular speed of the GIM mobile machine, comparison of this work with Wheel odometry data

B. Measuring all three components: Linear speed, angular speed, and sideslip speed

Figure 5 shows the linear, sideslip and angular speed of the GIM mobile machine while moving in a circular path on a frozen terrain. Figure 5(a) shows the comparison of linear speed computed using the proposed method and the wheel odometry. The wheel odometry does not calculate wheel slippage, therefore it is not considered to be accurate but still to get an idea of Radar sensor results, we have made this comparison. Figure 5(b) shows the sideslip speed. Lastly, in Figure 5(c), the angular speed computed using the gyroscope is presented.

C. Comparison to complete navigation solution

To measure the performance of the algorithm, we compare our proposed solution to a complete navigation solution, which uses wheel odometry, IMU, and Global Navigation Satellite System (GNSS). Dead reckoning trajectories are integration of following kinematic equation

$$^{W}\dot{\boldsymbol{r}}_B = {}^{W}\boldsymbol{R}_B \begin{bmatrix} v_B \\ v_d \end{bmatrix}$$

$$\dot{\phi} = \omega_B \qquad\qquad (9)$$

where $^{W}\boldsymbol{R}_B = \begin{bmatrix} cos\phi & -sin\phi \\ sin\phi & cos\phi \end{bmatrix}$ and ϕ is the heading angle of the GIM mobile machine, initialized by navigation solutions.

858

Input to dead reckoning, that is, (v_B, v_d, ω_B) directly comes from our algorithm.

The results are shown in Figure 6 (a, b) for X and Y directions. Figure 7 shows the proposed method (Radar odometry), wheel odometry and navigation data for X versus Y.
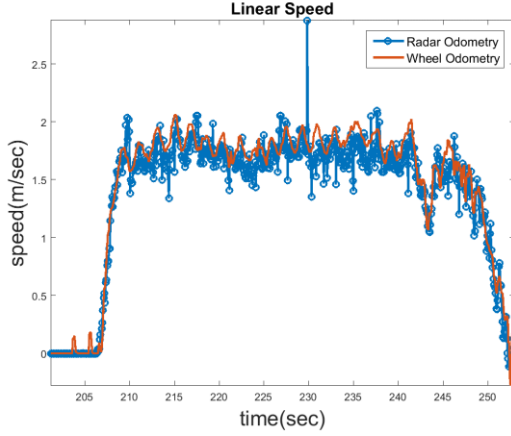

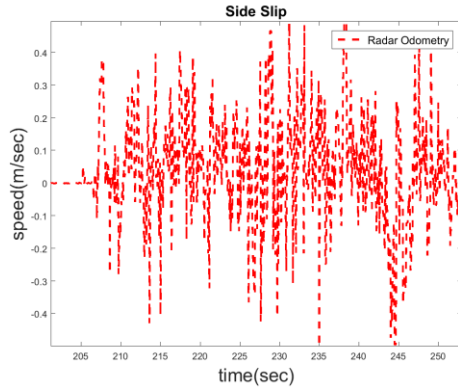Figure 5(a): Linear Speed of the GIM machine. Comparison of the proposed methods with Wheel odometry

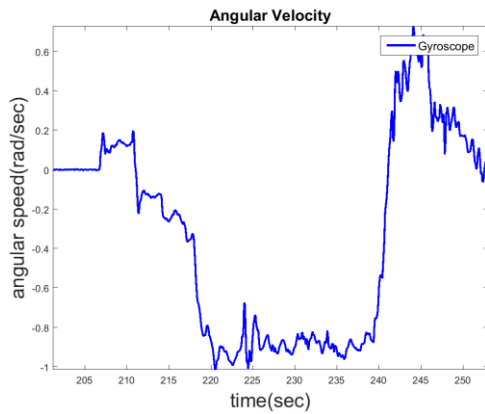Figure 5(b): Side Slip of the GIM machine while moving in a circular path with frozen terrain

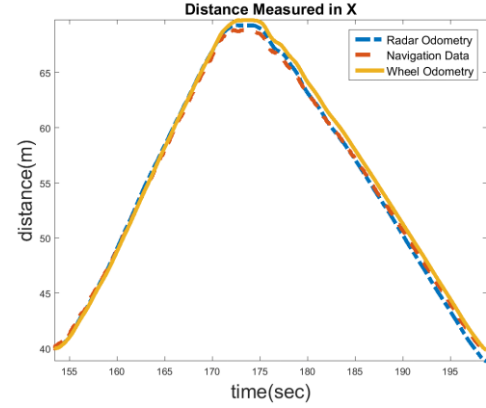Figure 5(c): Angular Speed of the GIM machine. Computed using gyroscope

Figure 6a: Distance measured by the Radar odometry, wheel odometry and the navigation data for X direction
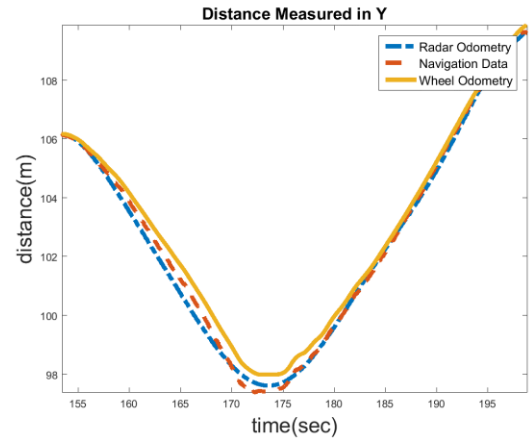

Figure 6b: Distance measured by the Radar odometry, wheel odometry and the navigation data for Y direction
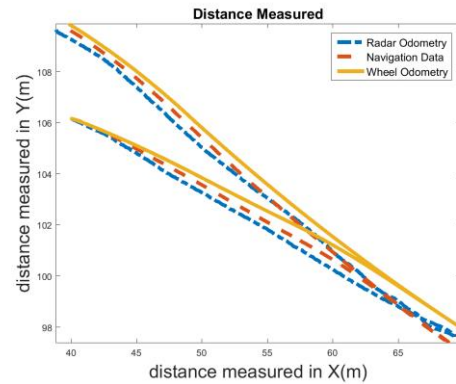

Figure 7: X distance vs Y distance. Measured by the Radar odometry, wheel odometry and the navigation data.

V. CONCLUSION

With a single Radar sensor together with a readily available IMU, the proposed algorithm is capable of calculating the linear forward and sideslip speeds, and angular speed of the machine in single measurement cycle. The results shows a feasible and alternative solution for any-vehicle odometry, especially more reliable compared to wheel odometry or to

visual odomtery in slippery ground and low visibility. Further improvements in several directions are needed to make the results usable in practice. For example, including variance of the measurement data in calculations, better outlier rejection, etc. More reliable results will then allow us to implement a complete navigation solutions and object mapping, leading to Radar SLAM (Simultaneous Localization and Mapping).

VI. Acknowledgment

The authors will like to thank the Laboratory of Automation and Hydraulics Engineering AUT/TUT for providing the GIM mobile machine for experiment purposes. The authors specially thank Dr. Mika Hyvönen and Antti Kolu for their technical support in system integration.

References

[1] "GIM - Finnish Centre of Excellence in Generic Intelligent Machines Research", Gim.aalto.fi, 2017. [Online]. Available: http://gim.aalto.fi/. [Accessed: 20- Feb- 2017].

[2] M. Aref, R. Ghabcheloo, A. Kolu, M. Hyvönen, K. Huhtala and J. Mattila, "Position-based visual servoing for pallet picking by an articulated-frame-steering hydraulic mobile machine", in 6th IEEE Conference on Robotics, Automation and Mechatronics (RAM), 2013.

[3] R. Ghabcheloo and M. Hyvönen, "Modeling and motion control of an articulated-frame-steering hydraulic mobile machine", in 17th Mediterranean Conference on Control & Automation, Makedonia Palace, Thessaloniki, Greece, 2009.

[4] R. Ghabcheloo, M. Hyvönen, J. Uusisalo, O. Karhu, J. Järä and K. Huhtala, "Automotive Motion Control of a Wheel Loader", in ASME 2009 Dynamic Systems and Control Conference, Hollywood, California, USA, 2009, pp. 427-434.

[5] P. Merriaux, Y. Dupuis, P. Vasseur and X. Savatier, "Wheel odometry-based car localization and tracking on vectorial map", in Intelligent Transportation Systems (ITSC), 2014 IEEE 17th International Conference, 2014.

[6] D. Vivet, P. Checchin and R. Chapuis, "Radar-only localization and mapping for ground vehicle at high speed and for riverside boat", in Robotics and Automation (ICRA), 2012 IEEE International Conference, 2014.

[7] J. Borenstein, H. Everett, L. Feng and D. Wehe, "Mobile robot positioning: Sensors and techniques", Journal of Robotic Systems, vol. 14, no. 4, pp. 231-249, 1997.

[8] D. Kellner, M. Barjenbruch, J. Klappstein, J. Dickmann and K. Dietmayer, "Instantaneous ego-motion estimation using Doppler Radar", in Intelligent Transportation Systems - (ITSC), 2013 16th International IEEE Conference, 2013.

[9] M. Rapp, M. Barjenbruch, K. Dietmayer, M. Hahn and J. Dickmann, "A fast probabilistic ego-motion estimation framework for Radar", in Mobile Robots (ECMR), 2015 European Conference, 2015.

[10] A. Corominas-Murtra, J. Vallvé, J. Solà, I. Flores and J. Andrade-Cetto, "Observability analysis and optimal sensor placement in stereo Radar odometry", in Robotics and Automation (ICRA), 2016 IEEE International Conference, 2016.

[11] M. Fischler and R. Bolles, "Random sample consensus: a paradigm for model fitting with applications to image analysis and automated cartography", Communications of the ACM, vol. 24, no. 6, pp. 381-395, 1981.

[12] C. Häne, T. Sattler and M. Pollefeys, "Obstacle Detection for Self-Driving Cars Using Only Monocular Cameras and Wheel Odometry", in IEEE/RSJ International Conference on Intelligent Robots and Systems (IROS), Hamburg, Germany, 2015.

[13] P. Checchin, F. Gérossier, C. Blanc and R. Chapuis, "Radar Scan Matching SLAM Using the Fourier-Mellin Transform", in Field and Service Robotics, 1st ed., Berlin/Heidelberg: Springer, 2017, pp. 151-161.

[14] D. Kellner, M. Barjenbruch, J. Klappstein, J. Dickmann and K. Dietmayer, "Instantaneous Ego-Motion Estimation using Multiple Doppler Radars", in 2014 IEEE International Conference on Robotics & Automation (ICRA), Hong Kong, 2014.